ARTICLE
Journal of Cellular Biochemistry 110:598–608 (2010)

Journal of Cellular Biochemistry

Cloning and Characterisation of GIRK1 Variants Resulting From Alternative RNA Editing of the KCNJ3 Gene Transcript in a Human Breast Cancer Cell Line

Valerie Wagner,[1] Elke Stadelmeyer,[2] Monika Riederer,[3] Peter Regitnig,[4] Astrid Gorischek,[1] Trevor DeVaney,[1] Kurt Schmidt,[5] Helmut A. Tritthart,[1] Koret Hirschberg,[6] Thomas Bauernhofer,[2] and Wolfgang Schreibmayer[1*]

[1]*Institute for Biophysics, Center of Physiological Medicine, Medical University of Graz, Graz, Austria*
[2]*Division of Oncology, Department of Internal Medicine, Medical University of Graz, Graz, Austria*
[3]*Institute for Molecular Biology and Biochemistry, Center of Molecular Medicine, Medical University of Graz, Graz, Austria*
[4]*Institute of Pathology, Medical University of Graz, Graz, Austria*
[5]*Department of Pharmaceutical Sciences, Karl Franzens Universität Graz, Graz, Austria*
[6]*Department of Pathology, Faculty of Medicine, Tel Aviv University, Tel Aviv, Israel*

ABSTRACT

The aim of this study was to investigate the impact of increased mRNA levels encoding GIRK1 in breast tumours on GIRK protein expression. mRNA levels encoding hGIRK1 and hGIRK4 in the MCF7, MCF10A and MDA-MB-453 breast cancer cell lines were assessed and the corresponding proteins detected using Western blots. cDNAs encoding for four hGIRK1 splice variants (hGIRK1a, 1c, 1d and 1e) were cloned from the MCF7 cell line. Subcellular localisation of fluorescence labelled hGIRK1a–e and hGIRK4 and of endogenous GIRK1 and GIRK4 subunits was monitored in the MCF7 cell line. All hGIRK1 splice variants and hGIRK4 were predominantly located within the endoplasmic reticulum. Heterologous expression in *Xenopus laevis* oocytes and two electrode voltage clamp experiments together with confocal microscopy were performed. Only the hGIRK1a subunit was able to form functional GIRK channels in connection with hGIRK4. The other splice variants are expressed, but exert a dominant negative effect on heterooligomeric channel function. Hence, alternative splicing of the KCNJ3 gene transcript in the MCF7 cell line leads to a family of mRNA's, encoding truncated versions of the hGIRK1 protein. The very high abundance of mRNA's encoding GIRK1 together with the presence of GIRK1 protein suggests a pathophysiological role in breast cancer. J. Cell. Biochem. 110: 598–608, 2010.

KEY WORDS: GIRK1; GIRK4; BREAST CANCER; MCF7; MCF10A

Tumour growth and metastasis is guided via complex signalling pathways, often located in the plasma membrane of malignant cells and their microenvironment [Steeg, 2006; Edwards et al., 2008]. Amongst these molecular players, hijacked by the malignant cell inducing and promoting vicious signalling circuits, are G-protein coupled receptors [GPCRs; Dorsam and Gutkind, 2007]. Ion channels are also increasingly recognised as playing an important role in this process [Pardo and Stuhmer, 2008; Shen et al., 2009; Sundelacruz et al., 2009]. Interestingly, both in the context with GPCR's and ion channels, G-protein activated inwardly rectifying potassium channels (GIRKs) represent a class of K^+ channels that link membrane potential to the presence of extracellular signalling molecules. This action is membrane delimited via GPCRs and pertussis toxin sensitive G-proteins. The role of GIRKs in neuronal cells and in the regulation of the heartbeat is well recognised [Dascal, 1997, 2001]. Evidence has accumulated that GIRKs also play roles in the regulation of other cellular activities, such as insulin secretion in the pancreas [Smith et al.,

Valerie Wagner and Elke Stadelmeyer contributed equally to the study.

*Correspondence to: Prof. Wolfgang Schreibmayer, Molecular Physiology Group, Institute for Biophysics, Center of Physiological Medicine, Medical University of Graz, Harrachgasse 21/4, A-8010 Graz, Austria.
E-mail: wolfgang.schreibmayer@medunigraz.at

Received 28 December 2009; Accepted 2 February 2010 • DOI 10.1002/jcb.22564 • © 2010 Wiley-Liss, Inc.
Published online 14 April 2010 in Wiley InterScience (www.interscience.wiley.com).

2001; Iwanir and Reuveny, 2008], blood platelet aggregation [Shankar et al., 2004, 2006] and regulation of lipid metabolism in fat cells [Perry et al., 2008]. Of interest for pathophysiological signalling during malignant neoplastic disease is the finding that mRNA levels encoding the GIRK1 subunit were heavily increased in primary breast carcinomas, when compared to healthy breast tissue. The increase in mRNA levels in the primary tumour was correlated with a higher incidence of lymph node metastases [Stringer et al., 2001]. Positive correlation between mRNA levels encoding GIRK1 and progression of disease was also found in non-small cell lung cancer, possibly indicating a general principle [Takanami et al., 2004]. Goal of the prevailing study was to investigate whether GIRK1 protein is expressed in breast cancer cells, to characterise the variants, their subcellular localisation and to test whether these proteins are able to form functional channels.

MATERIALS AND METHODS

QUANTIFICATION OF mRNA BY RT-PCR

Cells (1×10^7; 70–80% confluence) were homogenised (QIAshredder spin columns; Qiagen Gmbh, Hilden, Germany) and total RNA was isolated (RNeasy Mini Kit; Qiagen Gmbh). One microgram of total RNA was used for reverse transcription (QuantiTect Reverse Transcription Kit; Qiagen Gmbh). No amplification controls (NACs; no reverse transcriptase added) were used to check for the amplification of genomic DNA. Standard cRNAs were from human liver and spleen tissue. Aliquots of cDNA solution (equivalent to 100 ng RNA) were used for amplification of GIRK subtype-standards (QuantiTect SYBR Green PCR Kit; Qiagen Gmbh) with QuantiTect Primer Assays for GIRK1 (Hs_KCNJ3_1_SG), GIRK4 (Hs_KCNJ5_1_SG), and porphobilinogen deaminase (PBGD) as the housekeeping gene (Hs_HMBS_1_SG; Qiagen Gmbh). Reactions were run on a LightCycler 2.0 (50 cycles; Roche Diagnostics GmbH, Mannheim, Germany) and products checked on an agarose gel. Stock solutions of the purified dsDNA (QIAquick PCR Purification Kit; Qiagen Gmbh) and serial dilutions thereof served as standards. For the quantification of the hGIRK1 splice variants, primers spanning boundaries between different exons were designed (see Table I). In case of hGIRK1c + e, NACs served as control for contamination by genomic DNA. PCR reactions were carried out on a LightCycler 480 system using an equivalent of 20 ng RNA (45 cycles; Roche Diagnostics GmbH). PCR products were checked by gel electrophoresis and sequenced.

TABLE I. Primer Sequences Used for Quantification of mRNA Encoding Splice Variants of hGIRK1

Primer	Sequence	Amplicon size (bp)
GIRK1a fwd	5′-GTGGAAACAACTGGGATGAC-3′	137
GIRK1a rev	5′-GTTGCATGGAACTGGGAGTA-3′	
GIRK1c fwd	5′-GTTCGAGATTGTCGTCATCC-3′	142
GIRK1c rev	5′-CTCTGAGTCATTTCGCCCA-3′	
GIRK1d fwd	5′-CAAGCTGCTCAAAGGATGAC-3′	137
GIRK1d rev	5′-GTTGCATGGAACTGGGAGTA-3′	
GIRK1e fwd	5′-AACAGCCACATGGTCTCC-3′	252
GIRK1e rev	5′-ACAAGAGCACGAGAGTGAGT-3′	

CLONING OF cDNA ENCODING hGIRK1 SPLICE VARIANTS FROM THE MCF7 CELL LINE

mRNA was isolated from MCF7 cells and cDNA synthesised (PolyATtract System 1000; ImProm-II Reverse Transcription System; both from Promega, Madison, WI). PCR primers were designed based on known splice variants (in case when only the non-human sequence was available, the corresponding human chromosomal sequence was taken (NCBI Reference Sequence: NT_005403.16, Bethesda, MD)). The primers contained an additional nonamere for restriction and ligation into the Bluescript-MXT vector via the *Eco*RI/*Not*I sites (see Table II). The locations of the eight different regions on chromosome 2 are as follows (numbering according to NT_005403.16): region 1: 5764707–5765408; region 2: 5775534–5775749; region 3: 5920657–5921241; region 4: 5921244–5921555; region 5: 5913235–5913659; region 6: 5776379–5776747; region 7: 5765408–5765925; region 8: 5922388–5922432. cDNAs encoding splice variants were amplified using 35 cycles. PCR products were isolated from a preparative agarose gel, ligated into pBSmxt, transfected, amplified, and sequenced. The resulting clones were: hGIRK1a [sequence identical to Schoots et al., 1997], hGIRK1c (deposited at Genbank at GU068048), hGIRK1d (GU074515) and hGIRK1e (GU074516).

WESTERN BLOT ANALYSIS

Cell pellets were lysed on ice in RIPA buffer, using a Branson Digital Sonifier (model 250-D) for 20 s followed by ultracentrifugation at 50,000*g* (1 h; 4°C). Protein concentration in the supernatant was determined [Bradford, 1976]. Aliquots containing 50 μg protein were loaded onto 12% gels [Laemmli, 1970]. Following electrophoresis, proteins were transferred electrophoretically to nitrocellulose membranes (Hybond ECL, Amersham Biosciences; Amersham, Sweden). Membranes were blocked overnight with 5% non-fat dry milk in TBS (0.1% Tween-20; 4°C). Next, membranes were incubated with the primary antibody for 2 h and then incubated with the appropriate secondary antibody. Antibody–protein complexes were detected by the ECL plus Western Blotting Detection system (GE Healthcare, Amersham, Sweden).

ANTIBODIES

Primary antibodies. Rabbit antisera were raised against the recombinant protein comprising the rat GIRK1 (aa 183–501; 98.8% identity to the human sequence) and human GIRK4 (aa 178–374) C-termini that had been produced in bacteria as described [Müllner et al., 2009].

Secondary antibody. Peroxidase conjugated Affinity pure goat anti-rabbit IgG antibody (111-035-144, Jackson Immuno Research Laboratories, Suffolk, UK).

SOLUTIONS AND MEDIA (CONCENTRATIONS IN mMOL/L, UNLESS STATED OTHERWISE)

RIPA buffer: 50 Tris/HCl, 1% NP-40, 150 NaCl, 1 EDTA, 1 Na_3VO_4, 1 NaF plus protease inhibitors (P8340; Sigma Aldrich, Munich, Germany; 1 μl/ml) pH: 7.4. *TBS*: 10 Tris/Cl, 137 NaCl,

TABLE II. Reverse primer sequences of reverse primers used for the cloning of hGIRK1 splice variants

Primer	Sequence	Region	Exon	Insert amplified
hG1a_r	5′-TATGCGGCCGCTAAATAATGCCTAAGGGAGTGCTTTG-3′	3	3	hGIRK1a (1,576 bp), hGIRK1d (1,359 bp)
hG1c_r	5′-TATGCGGCCGCGAAACTTTATGGCATATCTGTTT-3′	2	2	hGIRK1c (994 bp)
hG1e_r	5′-TATGCGGCCGCCCTGTGGCTATAGGTAGAACCAGG-3′	7	1	hGIRK1e (860 bp)

0.1% Tween-20, pH: 7.4. *ND96*: 96 NaCl, 2 KCl, 1 $MgCl_2$, 1 $CaCl_2$, 5 HEPES, buffered with NaOH to pH: 7.4. *NDE*: same as ND96, but $CaCl_2$ was 1.8 and 2.5 pyruvate and 0.1% antibiotics (G-1397; 1000x stock from Sigma) were added; *HK*: 96 KCl, 2 NaCl, 1 $MgCl_2$, 1 $CaCl_2$, 5 HEPES buffered with KOH to pH: 7.4.

CELL CULTURE

Cell lines were from the American Type Culture Collection (ATCC, Manassas, VA) and cultured at 37°C and 5% CO_2.

CELL CULTURE MEDIA

MCF10A: MEBM (mammary epithelial basal medium), MEGM SingleQuot additives (Lonza Group Ltd, Basel, Switzerland), 100 ng/ml cholera toxin (Sigma Aldrich) and penicillin/streptomycin (100 U/ml and 100 ng/ml; PAA Laboratories GmbH, Pasching, Austria). *MCF12A*: 1:1 mixture of DMEM: F12 (ATCC; 30-2066), 20 ng/ml human endothelial growth factor (PeproTech, Hamburg, Germany), 100 ng/ml cholera toxin (Sigma Aldrich), 0.27 U/ml human insulin (Novo Nordisk, Vienna, Austria), 500 ng/ml hydrocortisone (Sigma Aldrich), 5% horse serum (Biochrom AG, Berlin, Germany) and penicillin/streptomycin (100 U/ml and 100 ng/ml, respectively). *MCF7*: MEM (PAA Laboratories GmbH), 10% foetal bovine serum (FBS 'Gold', PAA Laboratories GmbH), 1 mmol/L sodium pyruvat (PAA Laboratories GmbH) and penicillin/streptomycin (100 U/ml and 100 ng/ml). *MDA-MB-453*: Leibovitz's L-15 medium (Invitrogen, Karlsruhe, Germany), 10% or 20% FBS 'Gold' (PAA Laboratories GmbH) and penicillin/streptomycin (100 U/ml and 100 ng/ml). *SKBR3*: RPMI-1640 (Invitrogen, Karlsruhe, Germany), 10% FBS 'Gold' (PAA Laboratories GmbH) and penicillin/streptomycin (100 U/ml and 100 ng/ml). *T47D*: RPMI-1640 (ATCC; 30-2001), 10% FBS (ATCC; 30-2020), 0.2 U/ml recombinant human insulin (Novo Nordisk) and penicillin/streptomycin (100 U/ml and 100 ng/ml).

XENOPUS OOCYTE EXPRESSION

Oocytes were isolated as described previously [Hofer et al., 2006]. Fifty nanolitres of cRNA solution was injected per oocyte at the following concentrations (ng/μl): hGIRK1a(c,d,e): 2–50; hGIRK4: 1; mGIRK2: 1–250; hGIRK1a(c,d,e)^{eGFP}: 250; hGIRK4^{DsREd2}: 50; m_2R: 30. Oocytes were incubated in NDE for 4–6 days at 19°C. For the generation of fluorescence labelled chimeras, the coding sequence of the hGIRK1 splice variants were amplified from the original plasmids with primers containing *Eco*RI/*Not*I restriction sites, PCR products cloned into pBSNG (Genbank Acc. No.: EU022744) and the resulting plasmids sequenced. The resulting tagged proteins contain eGFP at their N-terminus. A similar vector based on a variant of the red fluorescence protein of *Discosoma* sp. (DsRed2) was used for hGIRK4. Plasmids were grown in bacteria, isolated, and linearised with *Sal*I using standard procedures [Sambrook and Russell, 2001]. cRNA was synthesised using T3 RNA-polymerase [Dascal, 1992].

ELECTROPHYSIOLOGY

Oocytes were placed in a recording chamber and superfused with either ND96 or HK (eventually containing 10^{-5} mol/L acetylcholine) at 21°C. Currents were recorded via the two electrode voltage clamp technique (TEVC) using agarose cushion electrodes (ACE; [Schreibmayer et al., 1994]) and the Geneclamp 500 amplifier (Axon Instr., USA). While the membrane potential was kept at −80 mV, superfusion was changed in the following order: ND96 → HK → HK + 10^{-5} mol/L acetylcholine → HK → ND96. The resulting changes in current were measured (I_{HK} and I_{ACh}; see Fig. 7A). Currents of a given experimental day and batch of oocytes were normalised to the average I_{HK} of the group injected with hGIRK1a/hGIRK4 (or hGIRK1a^{eGFP}/hGIRK4^{DsRed2}, respectively) plus m_2R. Current traces were low pass filtered at 10 Hz and digitised using the Digidata 1322A interface (Axon Instr.) connected to a MS-Windows compatible computer running the PClamp 9.2 software (Axon Instr.).

HETEROLOGOUS EXPRESSION IN THE MCF7 CELL LINE

Using the original plasmids as template (and primers containing *Xho*I/*Eco*RI restriction sites), the coding regions of hGIRK1a(c,d,e) and hGIRK4 were amplified by the PCR and cloned into the pEYFP-C1 and pECFP-C1 vectors, respectively (Clontech Laboratories, Inc., Mountain View, CA). The resulting inserts encoded chimeric proteins with the eYFP (or eCFP) at the N-terminus. Mammalian expression vectors encoding chimaeras between eCFP and protein domains with exclusive subcellular distributions were used in order to label different organelles *in vivo* (*lipid rafts within the plasma membrane*: glycosylphosphatidylinositol GpI^{eCFP} [Glebov and Nichols, 2004], *golgi apparatus*: galactosyl transferase Gal-T^{eCFP} [Ward et al., 2001], *lysosomes*: CD63^{eCFP} [Betzig et al., 2006], *endoplasmic reticulum*: Srβ^{eCFP} [Ward and Brandizzi, 2004]). Twenty-four hours to 56 h before confocal microscopy, MCF7 cells were transfected with the Transfast^{TM} transfection reagent (Promega).

CONFOCAL MICROSCOPY

Oocytes were scanned in ND96 using a Leica inverted microscope with a laser-scanning module attached (DMIRE2 and TCS SL2; Leica Microsystems, Heidelberg, Germany). Using the 20× (NA: 0.50) water immersion objective, confocal sections at 12 bit resolution (512 × 512 pixels) from a region slightly below the 'equator' of the

oocyte were obtained. Instrument settings, that is sensitivity of the PMT's, laser intensity and pinhole, were left constant for a given experimental day. Filter settings for fluorophore excitation and detection were: *DsRed2*: excitation (543 nm); excitation beam splitter TD 488/543/633; emission (570–635 nm); *eGFP*: excitation (488 nm); excitation beam splitter TD 488/543/633; emission (500–530 nm). Fluorescence intensities in defined regions of interest were measured and corrected for interference between the eGFP and DsRed2 channels, which ranged between 0.047–0.138 (eGFP to DsRed2) and 0.023–0.044 (DsRed2 to eGFP), depending on instrument settings. For every experimental day the eGFP fluorescence was normalised to the group solely expressing hGIRK1a^{eGFP}, while the DsRed2 fluorescence was normalised to the group solely expressing hGIRK4^{DsRed2}. For MCF7 cells the 63× (NA: 1.20) water immersion objective was used. Filter settings: *eYFP*: excitation (514 nm); excitation beam splitter: DD 458/514; emission (540–570 nm). *eCFP*: excitation (458 nm); excitation beam splitter: DD 458/514; emission (477–500 nm). Interference between eCFP and eYFP channels was negligible.

IMMUNOHISTOCHEMISTRY

Cell lines were fixed in 4% formalin, embedded in agar gel and histo-processed for paraffin-embedding. In addition a tissue microarray with breast carcinomas was tested. Tissue blocks of the breast carcinoma and the embedded cell lines were cut into 4-μm-thick sections and mounted on precoated slides. Sections were deparaffinised, rehydrated, and rinsed in distilled water. A Dako Real™ Detection System (Dako, Glostrup, Denmark) in conjunction with an indirect streptavidin–biotin method was used. Antigen retrieval was achieved by microwave heating in sodium citrate buffer pH 6.0 (40′). One hundred μL Dako Real™ Peroxidase Blocking Solution (Dako) was used, followed by incubation with the primary antibody (60′; KIR3.1(G-15), Santa Cruz Biotechnology, Inc., Santa Cruz, CA) 1:50 and KIR3.4(A-14) Santa Cruz, 1:50. A cross-species antibody rabbit-anti-goat was used (goat IgG-Fc cross adsorbed antibody, Bethyl Laboratories, Inc., Montgomery, TX) 1:1,000 for 30′, followed by incubation with the cross antibody, incubation with Dako Real™ biotinylated link antibody (Dako; 15′) and streptavidin HRP (Dako; 15′). One hundred μL of substrate chromogen solution diaminobenzidine (DAB) were added for 10 min. All slides were counterstained with haematoxylin, dehydrated, and mounted after xylol treatment with Entellan (Merck, Darmstadt, Germany).

BIOINFORMATICS AND STATISTICS

Sequence analysis and alignments were performed using GCG (Version 11.1, Accelrys, Inc., San Diego, CA). Analysis of confocal images was done using the ImageJ software (ImageJ 1.42 h by Wayne Rasband, NIH, Bethesda, MD) supported with deconvolution plugins (Bob Dougherty; http://www.optinav.com/imagej.html). Experimental parameters were checked for significant differences between groups using Student's *t*-test (Sigmaplot for Windows, v11, Systat Software, Inc., Chicago, IL).

RESULTS

QUANTITATIVE ANALYSIS OF mRNA

mRNA encoding hGIRK1 has been identified in several cancer cell lines, including lines derived from breast tumours [Plummer et al., 2004, 2005]. The RT-PCR experiments in the studies performed on the cancer cell lines did, however, not provide a quantitative analysis of mRNA levels. Hence it was of interest to analyse exact mRNA levels in the malignant MCF7 and MDA-MB-453 cell lines and compare them to the levels in the benign MCF10A breast epithelial cell line. Interestingly, the MCF7 cell line displayed mRNA levels encoding hGIRK1, that were orders of magnitude above the ones found in the other two cell lines (this mRNA species being almost absent in the MCF10A line). mRNA levels encoding hGIRK4, on the other hand, were low and comparable in the three cell lines studied (Fig. 1).

WESTERN BLOT ANALYSES

Despite the important pathophysiological implications that hGIRK1 protein expression may have in breast cancer, only sparse data exist on actual hGIRK1 protein expression. Therefore, protein expression of hGIRK1 and hGIRK4 was traced by Western blot analyses in several malignant (MCF7, MDA-MB-453, SKBR3, T47D) as well as in two breast epithelial cell lines (MCF10A, MCF12A; Fig. 2). hGIRK1 protein heterologously expressed in *Xenopus laevis* oocytes was taken as standard, in order to be able to exactly localise the hGIRK1

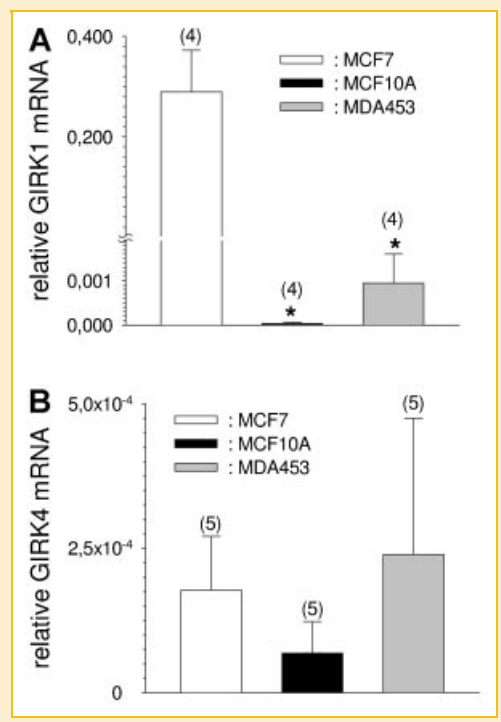

Fig. 1. Quantification of mRNA encoding hGIRK1 and hGIRK4 in different breast cancer cell lines. A: Copies of mRNA encoding GIRK1 per copy of the housekeeping gene (porphobilinogen deaminase—PBGD). B: Same as A, but for GIRK4 mRNA.

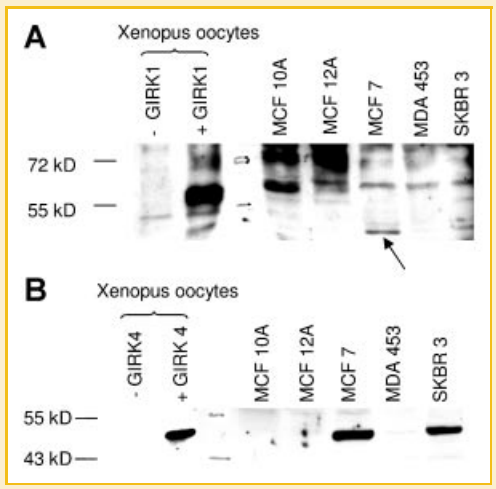

Fig. 2. Western blot analysis of GIRK1 and GIRK4 expression in different cell lines. A: The membrane was probed with the GIRK1 specific antibody. hGIRK1 heterologously expressed in *Xenopus* oocytes was used as a molecular ruler to identify GIRK1 (−GIRK1: control; +GIRK1: hGIRK1 co-expressed). B: The membrane was probed with the GIRK4 specific antibody. hGIRK4 heterologously expressed in *Xenopus* oocytes was used as a molecular ruler to identify GIRK4 (−GIRK4: control; +GIRK4: hGIRK4 co-expressed).

protein bands. Interestingly, highest amounts of the hGIRK1 protein were found in the two breast epithelial cell lines, but smaller amounts could be found in the malignant cell lines also. In the MCF7 cell line an additional, prominent but lower molecular weight band was detected (highlighted by the arrow in Fig. 2A), indicating a proteolytic fragment of the fully sized hGIRK1 protein or a smaller form of the protein, resulting from alternative splicing (see Table IV for summary of results). In line with our observations are the findings of Dhar and Plummer [2006], who had been unable to detect substantial amounts of the full-sized hGIRK1 protein in malignant breast cancer cell lines, including MCF7, MDA-MB-468, MDA-MB-453 and ZR-75-I, while significant amounts of a considerably smaller, GIRK1 antibody positive, protein had been detected (benign breast epithelial cell lines were not included in this study).

CLONING OF hGIRK1 SPLICE VARIANTS FROM MCF7 CELLS

The human KCNJ3 gene is located on chromosome 2 [Stoffel et al., 1994], its exon/intron organisation spanning at least 157 kb. The minimum number of exons in humans is 3 [Schoots et al., 1997]. Molecular cloning of GIRK1 related cRNA's from different species resulted so far in the discovery of five distinct splice variants, not all of them proven to exist in humans [Nelson et al., 1997; Stringer et al., 2001; Zhu et al., 2001; Steinecker et al., 2007]. Eight distinct regions within the humane genome correspond to these sequences (Fig. 3A,B; see the Materials and Methods Section for detailed explanation). Seven of these regions lie within or are directly connected to exons 1, 2 or 3. One of these regions, region 5, represents a putative additional, alternative exon and hence was denoted exon 3b in Figure 3A. We were able to isolate clones corresponding to four different splice variants 1a, 1c, 1d and 1e from

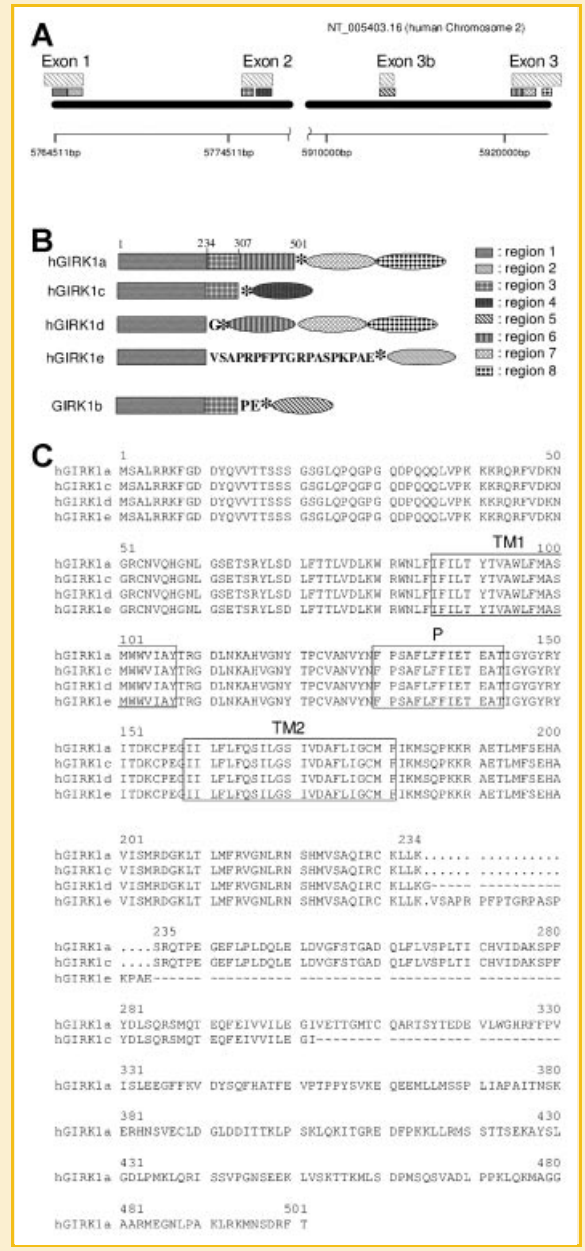

Fig. 3. Nucleotide and protein sequence of the different variants and chromosomal localisation of exons. A: Localisation of the different exons of the KCNJ3 gene on chromosome 2. The different regions, used for the design of the primers are also shown. B: Splice products of the KCNJ3 gene, as identified in the MCF7 cell line. The origin of the RNA from the different regions of the chromosome are shown (regions 1, 3 and 6 correspond to exons 1, 2 and 3, respectively). Rectangles denote open reading frames, ellipsoids untranslated regions. Single amino acids preceding the stop codon (marked by asterisks) are also shown. The hypothetical composition of GIRK1b, which was not found in the human MCF7 cell line, is shown at the bottom. C: Alignment of the deduced amino acid sequence of the splice variants. TM1, TM2 and P denote the two transmembrane regions and the pore region, respectively.

MCF7 cells. hGIRK1c and hGIRK1e have not been reported previously to occur in humans. The hypothetical splice variant 1b, described from rat, was shown to be absent in the MCF7 cell line. Translation of the open reading frames results in proteins that all

TABLE III. Splice Variants of cRNA Encoding hGIRK1 in the MCF7 Cell Line

Splice variant	1a	1b	1c	1d	1e
Copies	0.100/0.105	0.000/0.000	0.012/0.012	0.008/0.008	0.011/0.012
% Total	61.1%	0.0%	6.9%	25.3%	6.7%

The number of cDNA copies of a given splice variant per copy of the housekeeping gene (PBGD) was determined by two separate RT-PCR's. The contribution of a given splice variant to the total amount of hGIRK1 cDNA is also shown (% total).

comprise of two transmembrane helices and the characteristic pore structure (Fig. 3C). The size and calculated molecular weight of hGIRK1a is 501 amino acids and 56.6 kDa, 308 aa and 35.0 kDa for hGIRK1c, 235 aa and 26.8 kDa for hGIRK1d and 253 aa and 28.7 kDa for hGIRK1e, respectively. Quantitative RT-PCR revealed, that mRNA encoding hGIRK1a is the most abundant species in MCF7 cells, followed by hGIRK1d, hGIRK1c and hGIRK1e (Table III).

SUBCELLULAR LOCALISATION OF THE SPLICE VARIANTS IN THE MCF7 CELL LINE

In order to investigate whether the splice variants are properly synthesised in human cancer cells and to detect their subcellular localisation, N-terminal fusions (with respect to GIRK) with the enhanced cyan and yellow fluorescence proteins (eCFP and eYFP) were constructed and expressed in MCF7. Previous studies have shown that the GIRK4 subunit alone is readily able to localise in the plasma membrane of mammalian cells, while GIRK1 requires the association with GIRK4 or GIRK2 for membrane localisation [Ma et al., 2002]. The subcellular localisation of hGIRK1a^{eYFP} in MCF7 cells is shown in Figure 4. Interestingly, hGIRK1a^{eYFP} expressed alone is able to localise to the membrane, quite similar to hGIRK4^{eYFP} itself, indicating that endogenous GIRK4 subunits, as detected by our Western blot analysis (Fig. 2 and Table IV), suffice for surface localisation of GIRK1. Upon hGIRK1a^{eYFP}/hGIRK4^{eCFP} co-expression, both subunits co-localise strictly. Only small amounts of either the GIRK1 or the GIRK4 subunit localise to the surface. This is the case both for heterooligomeric hGIRK1a^{eYFP}/hGIRK4^{eCFP} and also for homooligomeric hGIRK1a^{eYFP} or hGIRK4^{eCFP} channels. In any case, the major fraction of both subunits remains within the cell. Small fractions of the hGIRK1a^{eYFP} protein, eventually comparable to the fraction at the surface, co-localise with the Golgi system and lysosomes. Similar results as described above were also obtained for the hGIRK1c-e^{eYFP} variants (data with all subcellular markers, except the ER are not shown here). As seen in Figure 5 for all the different splice variants, most of the hGIRK1a-e^{eYFP} protein localises to the endoplasmic reticulum, providing an enormous pool of protein for trafficking to the surface or other organelles.

TABLE IV. GIRK1 and GIRK4 Protein Detected by Western Blot Analysis

	GIRK1			GIRK4	
Cell line	Small size	Full length	N		N
MCF7	+	(+)	12	+	8
MDA-MB-453	(+)	(+)	8	(+)	7
SKBR3	+	(+)	10	+	8
MCF10A	−	+	13	−	8
MCF12A	−	+	7	−	4
T47D	+	(+)	4	+	4

+: Band clearly detectable. (+): Band faint, but detectable. −: Band was not detected. N: Number of individual experiments.

IMMUNOHISTOCHEMISTRY

hGIRK1 and hGIRK4 immunoreactivity was detectable in MCF7 and in human invasive breast carcinoma (Fig. 6). GIRK1 localisation is visible in cytoplasm and nuclei of tumour cells and barely visible on the cytoplasmic surface. The nuclear localisation was not seen upon heterologous expression of hGIRK1a–e^{eYFP}, and might be due to non-specific immunoreactivity. GIRK4 was similar, the nuclei of the breast carcinoma specimen also showing slight immunoreactivity.

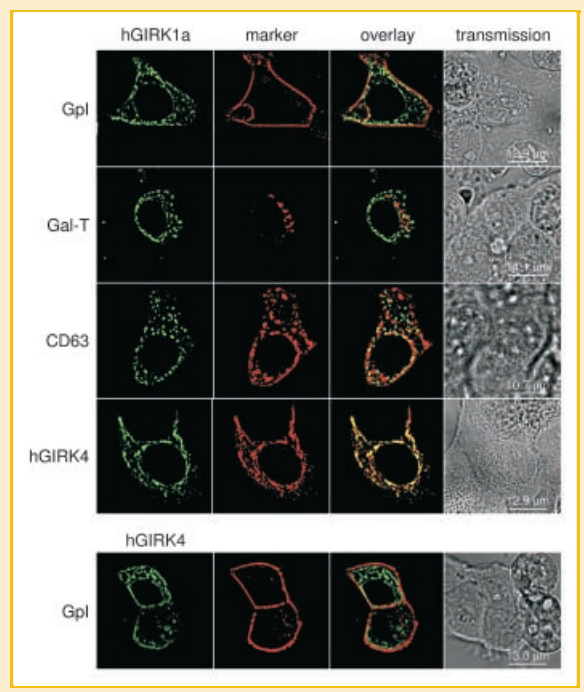

Fig. 4. Subcellular localisation of hGIRK1a^{eYFP} in MCF7 cells. Each horizontal sequence of images shows the same cell. The sequence of channels (from left to right) is: 1: eYFP; 2: eCFP; 3: overlay of eYFP and eCFP; 4: transmission. For better visualisation of co-localisation, the eYFP and eCFP channels are shown in *green* and *red*, respectively, hence *yellow* in the overlay image indicates co-localisation. The subcellular marker used is indicated at the left side of each horizontal series of images. The images at the bottom series show the co-localisation of hGIRK4^{eYFP} with Gpl^{eCFP}.

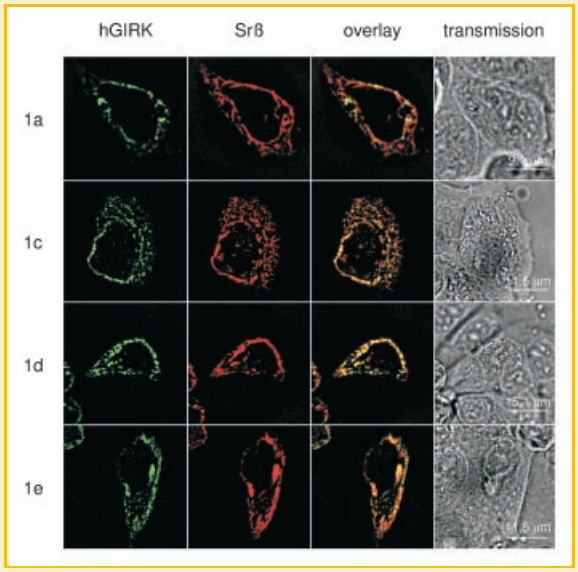

Fig. 5. Co-localisation of the different hGIRK1^{eYFP} splice variants with the endoplasmic reticulum. Each horizontal sequence of images shows the same cell. The sequence of channels is (left to right): 1: eYFP; 2: eCFP; 3: overlay of eYFP and eCFP; 4: transmission. For better visualisation of co-localisation, the eYFP and eCFP channels are shown in *green* and *red*, respectively. The subcellular marker used for all cells was Srβ^{eCFP}. The specific hGIRK1^{eYFP} splice variant used is indicated at the left side of each horizontal series.

Hence, a subcellular localisation pattern, similar to hGIRK1a–e^{eYFP} and hGIRK4^{eYFP}, was observed for native GIRK1 and GIRK4 protein, both in the MCF7 cell line and in individual breast cancer specimen.

FUNCTIONAL CHARACTERISATION OF THE SPLICE VARIANTS IN XENOPUS OOCYTES

Substantial agonist induced currents were recorded only from oocytes injected with the hGIRK1a splice variant (Fig. 7). As expected, co-expression of the hGIRK4 subunit potentiated basal as well as agonist induced currents produced by hGIRK1a. In the case of hGIRK1c, hGIRK1d or hGIRK1e, however, small but detectable

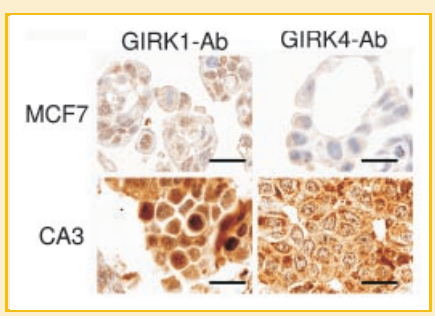

Fig. 6. Immunohistochemistry of native hGIRK1 and hGIRK4 channels. Top: MCF7 cells. hGIRK1 and hGIRK4 were stained with GIRK1 and GIRK4 specific antibodies, respectively (scale bar in each micrograph corresponds to 25.0 μm). *Bottom*: Same as above, but in a human breast carcinoma specimen (CA3).

agonist induced currents were recorded upon hGIRK4 co-expression. These currents were comparable in size to the ones recorded from oocytes injected with hGIRK4 alone, suggesting that they were produced by hGIRK4 homooligomeric channels. $G_{\beta/\gamma}$ binding sites are known to exist in the cytosolic C-terminus of hGIRK1a [Ivanina et al., 2003]. Therefore, truncated splice variants may be devoid of G-protein activation, but still may form constitutively active, agonist insensitive, K^+ channels. This is not the case for hGIRK1c, hGIRK1d and hGIRK1e, since I_{HK} was comparable to control oocytes in all cases (injected alone or in combination with hGIRK4). Even a 25× increase in the amount of RNA encoding hGIRK1c, hGIRK1d and hGIRK1e injected did not increase I_{HK} or I_{ACh} produced by hGIRK1c–e. Also co-expression of the mouse mGIRK2 subunit was ineffective in producing functional channels with hGIRK1c, hGIRK1d and hGIRK1e while, as expected, hGIRK1a potentiated both I_{HK} and I_{ACh} (data not shown). Inefficient translation may be responsible for the failure of the cRNA's encoding the smaller hGIRK1 variants to form functional K^+ channels. Therefore, both protein levels and GIRK function were quantified via the expression of fluorescence labelled versions of hGIRK1a–e (eGFP attached to the hGIRK1 N-terminus) and TEVC measurements in individual oocytes. The chimerical hGIRK1's were expressed alone or together with hGIRK4^{DsRed2} (hGIRK4 labelled with DsRed2 at its N-terminus; see Fig. 8). hGIRK1a^{eGFP} alone was able to form agonist induced functional K^+ channels, while co-expression of hGIRK4^{DsRed2} greatly potentiated the current. In the experiments with the fluorescence labelled GIRK subunits, 50× greater amounts of cRNA encoding hGIRK4^{DsRed2} were injected (compared to hGIRK4). Therefore, also currents through homooligomeric hGIRK4^{DsRed2} proteins were clearly measurable in this case. hGIRK1c^{eGFP}, hGIRK1d^{eGFP} and hGIRK1e^{eGFP} co-expression substantially reduced I_{ACh} in oocytes that expressed hGIRK4^{DsRed2}, indicating assembly of the short hGIRK1 variants with hGIRK4 resulting in inactive channels or channels with low open probability. Even in oocytes that expressed solely hGIRK1c–e^{eGFP} subunits, the residual petite I_{ACh}'s (presumably through endogenous frog fGIRK5 channels [Hedin et al., 1996]), were significantly reduced when compared to control oocytes (only m_2-receptors expressed; Fig. 8B). On the protein level, relative expression of hGIRK1a–e^{eGFP} and hGIRK4^{DsRed2} was clearly correlated in individual oocytes (Fig. 8C). Generally, hGIRK1a^{eGFP} expression was higher at a given level of hGIRK4^{DsRed2} expression, when compared to the short hGIRK1c–e^{eGFP} variants. The average hGIRK1^{eGFP} expression levels of the short variants were reduced approximately 4.1× to 10.8×, when compared to the control group, both when expressed alone or in combination with hGIRK4^{DsRed2} (see Table V for overview). Correlation of protein expression levels and agonist induced currents in 3 dimensions (Fig. 8D) reveals that I_{ACh} in oocytes expressing both hGIRK1a and hGIRK4 depends on GIRK4 *and* on GIRK1a expression. As expected, I_{ACh} does not depend on GIRK1a expression in oocytes expressing hGIRK1a alone, since the endogenous fGIRK5 is limiting [Hedin et al., 1996]. In oocytes expressing only the GIRK4 subunit, I_{ACh} correlates with the amount of hGIRK4 expressed. Upon hGIRK4^{DsRed2}/hGIRK1c^{eGFP} co-expression, I_{ACh} generally correlates only with hGIRK4 levels, that are however smaller, when compared to hGIRK4 ^{DsRed2} alone (shown

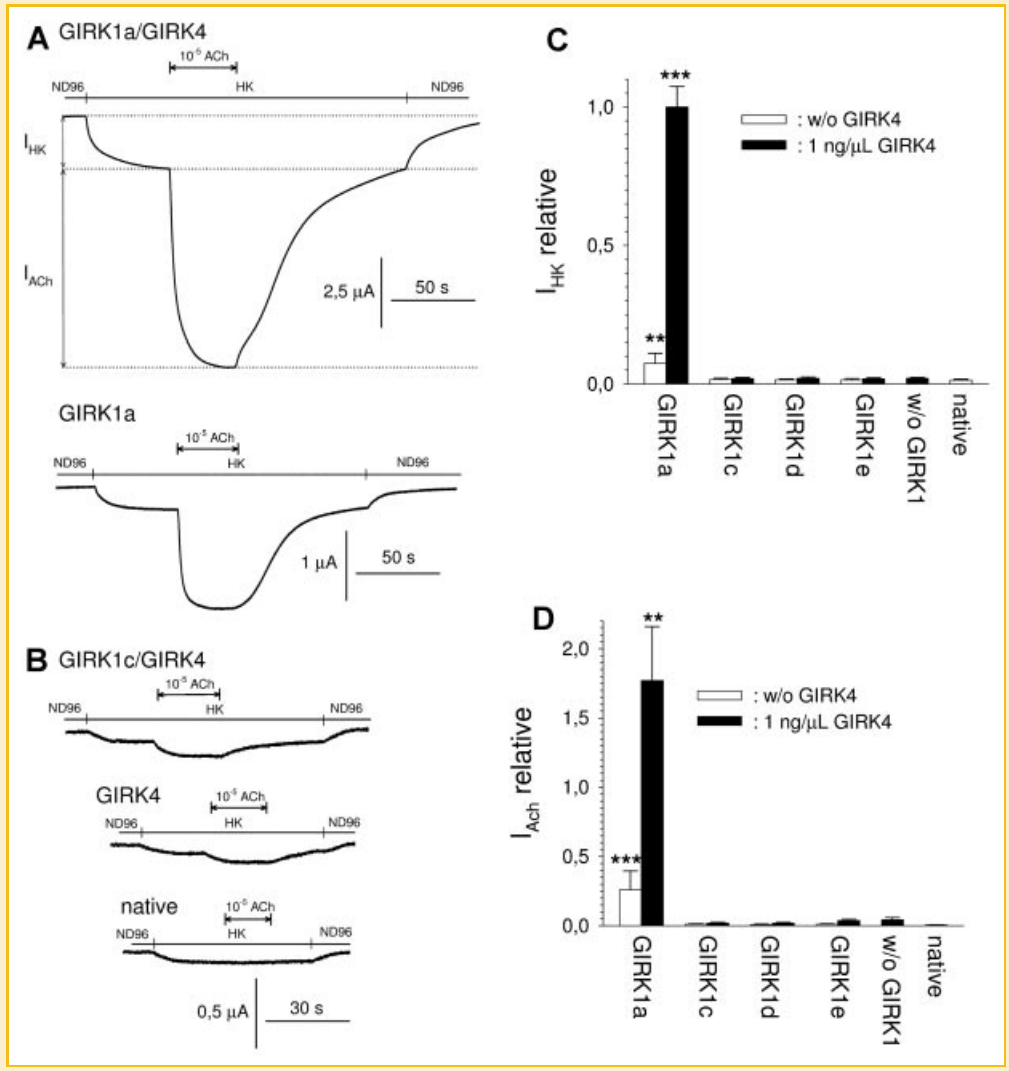

Fig. 7. Heterologous expression and TEVC on oocytes expressing GIRK1 splice variants. A: Top: Original current recording from an oocyte injected with hGIRK1a/hGIRK4 at a holding potential of −80 mV. The basal K^+ current (I_{HK}) is the current produced by a change of the extracellular medium from ND96 to HK. The agonist induced current (IA_{Ch}) is the current produced by activation of co-expressed m_2R's with 10^{-5} mol/L acetylcholine. Bottom: Same as above, but the oocyte expressed hGIRK1a alone. B: Original current recordings from oocytes expressing hGIRK1c/hGIRK4 (*top*), hGIRK4 alone (*middle*) and a native oocyte (*bottom*). Experimental paradigm as in A. C: Mean values of I_{HK}, relative to the control group (hGIRK1a/hGIRK4), from oocytes injected with the different hGIRK1 splice variants alone or in combination with hGIRK4. Data were derived from five different batches of oocytes (4–5 oocytes were measured per batch for each experimental group). **; ***: The mean value differs statistically significant from native oocytes at the $P < 0.01$; 0.001 level. D: Mean values of I_{ACh}, relative to I_{HK} of the control group (hGIRK1a/hGIRK4). Same oocytes as in C.

in Fig. 8D). Co-expression experiments with hGIRK1d^{eGFP} and hGIRK1e^{eGFP} gave similar results (not shown). Hence we are left with the conclusion that *both* low protein expression *and* formation of inactive heterooligomers account for the inability of hGIRK1c–e to produce functional channels.

DISCUSSION

A striking result of our study is that the level of KCNJ3 gene transcript is increased by several orders of magnitude in the malignant MCF7, when compared to the benign MCF10A cell line. Surprisingly, the amount of protein did not correspond with mRNA levels, as detected by Western blot analysis. The full-length protein (glycosylated and non-glycosylated) was even expressed more pronounced in the MCF10A (and MCF12A) cell line, while the corresponding mRNA was hardly detectable. In a recent, comprehensive, study the molecular features of 51 breast cancer cell lines (including the ones used in the present study) and 145 primary breast tumours were compared [Neve et al., 2006]. Western blot analysis was performed in 38 cell lines, using antibodies directed against 50 different proteins of interest (GIRK proteins were not amongst the ones tested): in only a subset of the proteins tested, the protein levels were directly correlated with mRNA levels. This finding demonstrates that caution must be taken when protein expression is deduced from the measurement of the mRNA level, as

these values often are uncorrelated. In another recent study [Brevet et al., 2008], a pronounced immunohistochemical staining of breast tumour specimen with GIRK1 antibody was found, but not of healthy tissue. A correlation of staining intensity and hence increased GIRK1 expression with prognostic outcome of the patients was found, suggesting that the increased mRNA levels may well result in increased protein expression. Based on our observations, we conclude that this increased immunostaining is mostly due to the shorter, non-full length, GIRK1 truncation that was heavily over-expressed in our Western blots, when compared to the MCF10A line. The different splice variants differ within their C-termini and the polyclonal antibody, used in the prevailing study, was directed against the entire GIRK1 C-terminus. Therefore it must be noted that it is theoretically possible that the staining of the shorter splice variants is weaker and hence their amounts were underestimated. The malignant MCF7, SKBR3 and T47D lines exerted high levels of expression of the truncated GIRK1 version, accompanied by high GIRK4 expression. Interestingly, GIRK4 co-expression is required for GIRK1 to form functional heterooligomeric K^+ channels [Krapivinsky et al., 1995]. The MCF10A and MCF12A cell lines, resembling healthy breast tissue in many molecular features, were the only ones that clearly expressed the full-length GIRK1 subunit, but no GIRK4 was present. Possibly another GIRK subunit exists in these cells, forming G-protein activated channels that are required for normal physiological function. During the course of neoplasia, full-length GIRK1 proteins disappear and the extremely high levels of GIRK1 mRNA may represent a form of active counter-regulation/compensation of the cell. The expression studies using fluorescent labelled chimeric hGIRK1a–e and GIRK4 showed reduced, but clearly detectable expression of the smaller hGIRK1c–e isoforms in *Xenopus* oocytes. Correct translation was also shown in the MCF7 cell line. Subcellular localisation of all hGIRK1 variants was

TABLE V. Expression of hGIRK1^{eGFP} and hGIRK4^{DsRed2} in *Xenopus* oocytes

Subunit combination	eGFP expression	DsRed2 expression	N
hGIRK1a^{eGFP}	100.0 ± 12.6%	/	29
hGIRK1c^{eGFP}	9.3 ± 4.3%***	/	29
hGIRK1d^{eGFP}	13.9 ± 3.2%***	/	29
hGIRK1e^{eGFP}	18.6 ± 2.9%***	/	24
hGIRK1a^{eGFP}/hGIRK4^{DsRed2}	66.2 ± 7.2%***	54.5 ± 9.2%***	24
hGIRK1c^{eGFP}/hGIRK4^{DsRed2}	13.5 ± 2.8%***	61.5 ± 8.1%***	24
hGIRK1d^{eGFP}/hGIRK4^{DsRed2}	10.4 ± 1.1%***	81.7 ± 12.7%	29
hGIRK1e^{eGFP}/hGIRK4^{DsRed2}	24.6 ± 3.3%***	79.0 ± 8.2%*	28
hGIRK4^{DsRed2}	/	100.0 ± 9.0%	30

Data were derived from three different batches of oocytes. Mean values ± SEM are shown. N denotes the number of individual oocytes that were scanned per group. */***: The mean value differs significantly at the $P < 0.05$/0.001 level from the control (hGIRK1a^{eGFP} for eGFP expression and hGIRK4^{DsRed2} for DsRed2 expression).

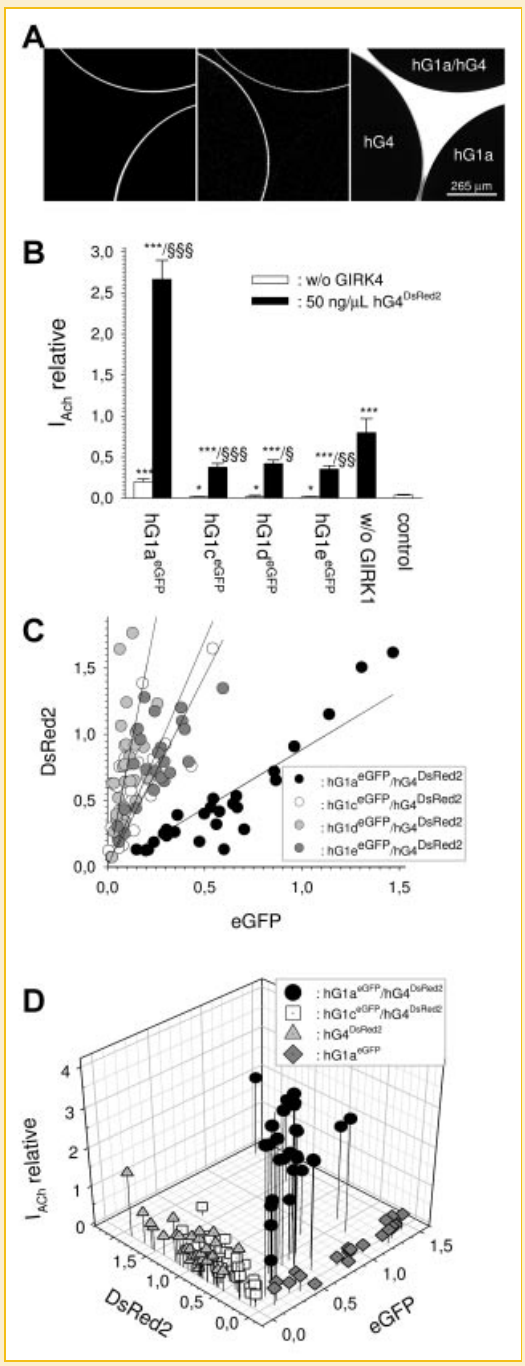

Fig. 8. Confocal microscopy and TEVC of oocytes expressing the hGIRK1a–e^{eGFP} and hGIRK4^{DsRed2} proteins. A: Confocal images obtained from three oocytes expressing hGIRK1a^{eGFP}/hGIRK4^{DsRed2}, hGIRK4^{DsRed2} and hGIRK1a^{eGFP}. Left: eGFP channel; middle: DsRed2 channel; right: transmission. B: Mean values of relative I_{ACh} from oocytes injected with the different hGIRK1^{eGFP} splice variants alone or in combination with hGIRK4^{DsRed2}. Data were derived from three different batches of oocytes (7–10 oocytes were measured per batch for each experimental group). $^{*;\ **;\ ***}$: The mean value differs statistically significant from the control group (oocytes expressing m_2R alone) at the $P < 0.05$; 0.01; 0.001 level. $^{§;\ §§;\ §§§}$: The mean value differs statistically significant from the group expressing hGIRK4^{DsRed2} alone at the $P < 0.05$; 0.01; 0.001 level. C: Individual levels of expression of oocytes expressing the different hGIRK1^{eGFP} splice variants in combination with hGIRK4^{DsRed2}. Solid lines denote linear regressions through the data of each experimental group. D: Correlation of individual hGIRK1^{eGFP} expression, hGIRK4^{DsRed2} expression and I_{ACh} in four selected experimental groups.

indistinguishable. Only a small fraction of the hGIRK1 protein surfaced to the plasma membrane, likely due to the endogenously existing GIRK4 subunits. The major fraction of hGIRK1 localised to the endoplasmic reticulum. In the MCF7 cell line and also in breast tumour specimen, the major fractions of native hGIRK1 and hGIRK4 proteins were located intracellularly. Interestingly in this context, intracellular localisation of the major fraction of GIRK1 protein was recently shown to occur also in neuronal cells, where regulation of the trafficking to the surface via protein phosphorylation was shown to affect neuronal plasticity and long-term potentiation [Chung et al., 2009a,b].

In the MCF7 cell line, alternative splicing of KCNJ3 transcript leads to a family of mRNA's encoding not only the full-length hGIRK1a variant, but also the shorter hGIRK1c, hGIRK1d and hGIRK1e isoform. When tested with conventional expression methods, only the hGIRK1a subunit was able to form functional channels, although the differences between variants refer to the cytosolic C-terminal region important for G-protein activation and phosphorylation [Müllner et al., 2009] and not to transmembrane regions including the K^+ pore. Instead of forming functional channels, the hGIRK1c–e variants exerted a dominant negative effect on heterooligomeric GIRK1/GIRK4 channel function thereby impairing G-protein signalling. Possibly, GIRK mediated G-protein signalling is required for physiological breast cell functioning and hence over-expression of splice variants mediates malignancy. As an alternative possibility, the shorter variants may contribute to K^+ channels that remain silent under the experimental conditions tested, but become activated under pathophysiological conditions and mediate cell proliferation.

Seventy-eight genes within the human genome encode α-subunits of K^+ selective ion channels. Besides their indispensable roles in shaping the action potential in electrically excitable cells, many of them have been identified as essential players in Ca^{2+} signalling, volume regulation, secretion, proliferation and migration of electrically non-excitable cells [see Shen et al., 2009; Wulff et al., 2009 for recent reviews]. Regarding the malignancy of cancer cells, K^+ channels have been shown to be crucially involved both via K^+ permeation [e.g. Pei et al., 2003; Voloshyna et al., 2008] as well as via moonlighting functions that are unrelated to K^+ permeation [e.g. Pardo, 2004; Afrasiabi et al., 2010]. Generally and unequivocally, a diversity of K^+ channel subunits has been identified to be of fundamental and vital importance for breast cancer cells [Coiret et al., 2005, 2007; Hemmerlein et al., 2006; vanTol et al., 2007; Ouadid-Ahidouch and Ahidouch, 2008; Roy et al., 2008]. Future studies will show the functional role(s) of GIRK proteins produced by the alternative splicing of the KCNJ3 gene in the pathophysiology of breast cancer cells.

ACKNOWLEDGMENTS

Financial support by the Research Foundation of the Austrian National Bank (OENB 12575) and by the county of Styria (GZ: A3-16.R-10/2009-112) is gratefully acknowledged.

REFERENCES

Afrasiabi E, Hietamaki M, Viitanen T, Sukumaran P, Bergelin N, Tornquist K. 2010. Expression and significance of HERG (KCNH2) potassium channels in the regulation of MDA-MB-435S melanoma cell proliferation and migration. Cell Signal 22:57–64.

Betzig E, Patterson GH, Sougrat R, Lindwasser OW, Olenych S, Bonifacino JS, Davidson MW, Lippincott-Schwartz J, Hess HF. 2006. Imaging intracellular fluorescent proteins at nanometer resolution. Science 313:1642–1645.

Bradford MM. 1976. Rapid and sensitive method for quantitation of microgram quantities of protein utilizing principle of protein-dye binding. Anal Biochem 72:248–254.

Brevet M, Ahidouch A, Sevestre H, Merviel P, El Hiani Y, Robbe M, Ouadid-Ahidouch H. 2008. Expression of K+ channels in normal and cancerous human breast. Histol Histopathol 23:965–972.

Chung HJ, Ge WP, Qian X, Wiser O, Jan YN, Jan LY. 2009a. G protein-activated inwardly rectifying potassium channels mediate depotentiation of long-term potentiation. Proc Natl Acad Sci USA 106:635–640.

Chung HJ, Qian X, Ehlers M, Jan YN, Jan LY. 2009b. Neuronal activity regulates phosphorylation-dependent surface delivery of G protein-activated inwardly rectifying potassium channels. Proc Natl Acad Sci USA 106:629–634.

Coiret G, Borowiec AS, Mariot P, Ouadid-Ahidouch H, Matifat F. 2007. The antiestrogen tamoxifen activates BK channels and stimulates proliferation of MCF-7 breast cancer cells. Mol Pharmacol 71:843–851.

Coiret G, Matifat F, Hague F, Ouadid-Ahidouch H. 2005. 17-beta-estradiol activates maxi-K channels through a non-genomic pathway in human breast cancer cells. FEBS Lett 579:2995–3000.

Dascal N. 1997. Signalling via the G protein-activated K+ channels. Cell Signal 9:551–573.

Dascal N. 2001. Ion-channel regulation by G proteins. Trends Endocrinol Metab 12:391–398.

Dascal NLI. 1992. Expression of exogenous ion channels and neurotransmitter receptors in RNA-injected Xenopus oocytes. In: Longstaff ARP, editor. Methods in neurobiology. Totowa, NJ: Humana Press. pp 205–225.

Dhar MS, Plummer HK. 2006. Protein expression of G-protein inwardly rectifying potassium channels (GIRK) in breast cancer cells. BMC Physiol 6:8.

Dorsam RT, Gutkind JS. 2007. G-protein-coupled receptors and cancer. Nat Rev Cancer 7:79–94.

Edwards CM, Zhuang JL, Mundy GR. 2008. The pathogenesis of the bone disease of multiple myeloma. Bone 42:1007–1013.

Glebov OO, Nichols BJ. 2004. Lipid raft proteins have a random distribution during localized activation of the T-cell receptor. Nat Cell Biol 6:238–243.

Hedin KE, Lim NF, Clapham DE. 1996. Cloning of a Xenopus laevis inwardly rectifying K+ channel subunit that permits GIRK1 expression of I-KACh currents in oocytes. Neuron 16:423–429.

Hemmerlein B, Weseloh RM, de Queiroz FM, Knotgen H, Sanchez A, Rubio ME, Martin S, Schliephacke T, Jenke M, Heinz Joachim R, Stuhmer W, Pardo LA. 2006. Overexpression of EagI potassium channels in clinical tumours. Mol Cancer 5. DOI: 10.1186/1476-4598-5-41.

Hofer D, Lohberger B, Steinecker B, Schmidt K, Quasthoff S, Schreibmayer W. 2006. A comparative study of the action of tolperisone on seven different voltage dependent sodium channel isoforms. Eur J Pharmacol 538:5–14.

Ivanina T, Rishal I, Varon D, Mullner C, Frohnwieser-Steinecke B, Schreibmayer W, Dessauer CW, Dascal N. 2003. Mapping the G beta gamma-binding sites in GIRK1 and GIRK2 subunits of the G protein-activated K+ channel. J Biol Chem 278:29174–29183.

Iwanir S, Reuveny E. 2008. Adrenaline-induced hyperpolarization of mouse pancreatic islet cells is mediated by G protein-gated inwardly rectifying potassium (GIRK) channels. Pflugers Arch 456:1097–1108.

Krapivinsky G, Gordon EA, Wickman K, Velimirovic B, Krapivinsky L, Clapham DE. 1995. The G-protein-gated atrial K+ channel I-Kach is a heteromultimer of 2 inwardly rectifying K+-channel proteins. Nature 374:135–141.

Laemmli UK. 1970. Cleavage of structural proteins during assembly of head of bacteriophage-T4. Nature 227:680–685.

Ma D, Zerangue N, Raab-Graham K, Fried SR, Jan YN, Jan LY. 2002. Diverse trafficking patterns due to multiple traffic motifs in G protein-activated inwardly rectifying potassium channels from brain and heart. Neuron 33:715–729.

Müllner CSB, Gorischek A, Schreibmayer W. 2009. Identification of the structural determinant responsible for the phosphorylation of GIRK1 by cAMP dependent proteinkinase. FEBS J 276(21):6218–6226.

Nelson CS, Marino JL, Allen CN. 1997. Cloning and characterization of Kir3.1 (GIRK1) C-terminal alternative splice variants. Brain Res Mol Brain Res 46:185–196.

Neve RM, Chin K, Fridlyand J, Yeh J, Baehner FL, Fevr T, Clark L, Bayani N, Coppe JP, Tong F, Speed T, Spellman PT, DeVries S, Lapuk A, Wang NJ, Kuo WL, Stilwell JL, Pinkel D, Albertson DG, Waldman FM, McCormick F, Dickson RB, Johnson MD, Lippman M, Ethier S, Gazdar A, Gray JW. 2006. A collection of breast cancer cell lines for the study of functionally distinct cancer subtypes. Cancer Cell 10:515–527.

Ouadid-Ahidouch H, Ahidouch A. 2008. K+ channel expression in human breast cancer cells: Involvement in cell cycle regulation and carcinogenesis. J Membr Biol 221:1–6.

Pardo LA. 2004. Voltage-gated potassium channels in cell proliferation. Physiology 19:285–292.

Pardo LA, Stuhmer W. 2008. Eag1: An emerging oncological target. Cancer Res 68:1611–1613.

Pei L, Wiser O, Slavin A, Mu D, Powers S, Jan LY, Hoey T. 2003. Oncogenic potential of TASK3 (Kcnk9) depends on K+ channel function. Proc Natl Acad Sci USA 100:7803–7807.

Perry CA, Pravetoni M, Teske JA, Aguado C, Erickson DJ, Medrano JF, Lujan R, Kotz CM, Wickman K. 2008. Predisposition to late-onset obesity in GIRK4 knockout mice. Proc Natl Acad Sci USA 105:8148–8153.

Plummer HK, Dhar MS, Cekanova M, Schuller HM. 2005. Expression of G-protein inwardly rectifying potassium channels (GIRKs) in lung cancer cell lines. BMC Cancer 5. DOI: 10.1186/1471-2407-5-104.

Plummer HK, Yu Q, Cakir Y, Schuller HM. 2004. Expression of inwardly rectifying potassium channels (GIRKs) and beta-adrenergic regulation of breast cancer cell lines. BMC Cancer 4. DOI: 10.1186/1471-2407-4-93.

Roy J, Vantol B, Cowley EA, Blay J, Linsdell P. 2008. Pharmacological separation of hEAG and hERG K+ channel function in the human mammary carcinoma cell line MCF-7. Oncol Rep 19:1511–1516.

Sambrook JR, Russell DW. 2001. Molecular cloning. 3rd edition. Cold Spring Harbour: CSH.

Schoots O, Voskoglou T, VanTol HHM. 1997. Genomic organization and promoter analysis of the human G-protein-coupled K+ channel Kir3.1 (KCNJ3/HGIRK1). Genomics 39:279–288.

Schreibmayer W, Lester HA, Dascal N. 1994. Voltage clamping of Xenopus-Laevis oocytes utilizing agarose-cushion electrodes. Pflugers Arch 426:453–458.

Shankar H, Kahner BN, Prabhakar J, Lakhani P, Kim S, Kunapuli SP. 2006. G-protein-gated inwardly rectifying potassium channels regulate ADP-induced cPLA(2) activity in platelets through Src family kinases. Blood 108:3027–3034.

Shankar H, Murugappan S, Kim S, Jin JG, Ding ZR, Wickman K, Kunapuli SP. 2004. Role of G protein-gated inwardly rectifying potassium channels in P2Y(12) receptor-mediated platelet functional responses. Blood 104:1335–1343.

Shen Z, Yang Q, You QD. 2009. Researches toward potassium channels on tumor progressions. Curr Top Med Chem 9:322–329.

Smith PA, Sellers LA, Humphrey PPA. 2001. Somatostatin activates two types of inwardly rectifying K+ channels in MIN-6 cells. J Physiol (London) 532:127–142.

Steeg PS. 2006. Tumor metastasis: Mechanistic insights and clinical challenges. Nat Med 12:895–904.

Steinecker B, Rosker C, Schreibmayer W. 2007. The GIRK1 brain variant GIRK1d and its functional impact on heteromultimeric GIRK channels. J Receptors Signal Transduct 27:369–382.

Stoffel M, Espinosa R, Powell KL, Philipson LH, Lebeau MM, Bell GI. 1994. Human G-protein-coupled inwardly rectifying potassium channel (GIRK1) gene (KCNJ3)—Localization to chromosome-2 and identification of a simple tandem repeat polymorphism. Genomics 21:254–256.

Stringer BK, Cooper AG, Shepard SB. 2001. Overexpression of the G-protein inwardly rectifying potassium channel 1 (GIRK1) in primary breast carcinomas correlates with axillary lymph node metastasis. Cancer Res 61:582–588.

Sundelacruz S, Levin M, Kaplan DL. 2009. Role of membrane potential in the regulation of cell proliferation and differentiation. Stem Cell Rev Rep 5:231–246.

Takanami I, Inoue Y, Gika M. 2004. G-protein inwardly rectifying potassium channel I (GIRK I) gene expression correlates with tumor progression in non-small cell lung cancer. BMC Cancer 4. DOI: 10.1186/1471-2407-4-79.

vanTol BL, Missan S, Crack J, Moser S, Baldridge WH, Linsdell P, Cowley EA. 2007. Contribution of KCNQ1 to the regulatory volume decrease in the human mammary epithelial cell line MCF-7. Am J Physiol Cell Physiol 293:C1010–C1019.

Voloshyna I, Besana A, Castillo M, Matos T, Weinstein IB, Mansukhani M, Robinson RB, Cordon-Cardo C, Feinmark SJ. 2008. TREK-1 is a novel molecular target in prostate cancer. Cancer Res 68:1197–1203.

Ward TH, Brandizzi F. 2004. Dynamics of proteins in Golgi membranes: Comparisons between mammalian and plant cells highlighted by photobleaching techniques. Cell Mol Life Sci 61:172–185.

Ward TH, Polishchuk RS, Caplan S, Hirschberg K, Lippincott-Schwartz J. 2001. Maintenance of Golgi structure and function depends on the integrity of ER export. J Cell Biol 155:557–570.

Wulff H, Castle NA, Pardo LA. 2009. Voltage-gated potassium channels as therapeutic targets. Nat Rev Drug Discov 8:982–1001.

Zhu LX, Wu XY, Wu MB, Chan KW, Logothetis DE, Thornhill WB. 2001. Cloning and characterization of G protein-gated inward rectifier K+ channel (GIRK1) isoforms from heart and brain. J Mol Neurosci 16:21–32.